

# Statistical Active-Sensing Structural Health Monitoring via Stochastic Time-Varying Time Series Models

Shabbir Ahmed and Fotis Kopsaftopoulos<sup>1</sup>

Intelligent Structural Systems Lab (ISSL)

Department of Mechanical, Aerospace and Nuclear Engineering  
Rensselaer Polytechnic Institute, Troy, NY.

**Abstract**—In the context of acousto-ultrasound guided wave-based damage diagnosis, the vast majority of existing methods are deterministic in nature and face significant challenges when exposed to real-life situations, potentially varying environmental and operating conditions, and stochastic time-varying structural response and uncertainty. These factors limit the applicability and widespread adoption of structural health monitoring (SHM) methods for aerospace, mechanical, and civil engineering systems. Thus, there lies a need for accurate and robust damage diagnosis methods for assessing the structural health under uncertainty. In this work, a novel statistical method for structural damage detection and identification, collectively referred to as damage diagnosis, via ultrasonic guided waves is postulated using stochastic time-varying time series models. Ultrasonic guided waves, that are dispersive in nature, are represented via recursive maximum likelihood time-varying autoregressive (RML-TAR) and functional series time-varying autoregressive (FS-TAR) models. Next, the estimated time-varying model parameters are employed within a statistical decision-making framework to tackle damage detection and identification under predetermined type I error probability levels. Both damage intersecting and non-intersecting paths are considered in a multi-sensor aluminum plate in pitch-catch configuration for the complete experimental assessment. The detailed damage diagnosis results are presented and the method's robustness, effectiveness, and limitations are discussed.

## I. INTRODUCTION

With the increasing interest in intelligent, self-aware systems, structural health monitoring (SHM) in mechanical, aerospace and civil structures offers a potential approach to enhance the safety, improve the performance, reduce maintenance cost, and enable the life-cycle monitoring and management [1], [2]. An SHM process involves automatic extraction of damage-sensitive quantities or features from continuous of periodic measurements coming from an array of permanently installed sensors on a structure/system and perform statistical analysis of these quantities to determine the current structural state of the system. In addition, SHM may enable the prognostic capabilities and estimation of the remaining useful service life, while also allowing for new approaches for structural control and life-cycle expansion.

Active sensing SHM approaches constitute an important family of SHM methods that are based on piezoelectric transducers, operating both as actuators and sensors, that generate ultrasonic guided waves on structural regions of

interest. Such methods are extremely sensitive to local structural changes and can detect tiny defects/damage within a structure [3]–[5]. The most widely used methods for damage detection using guided waves are based on the concept of damage/health indices/indicators (D/HI), where features of the signal for an unknown structural state are compared to that coming from the healthy structure. The features may be based on the specific mode wave packets of the guided wave, the amplitude/magnitude, time of flight, or the energy content of the signal. Such conventional DI-based approaches have been extensively used in the literature due to their simplicity and damage/no-damage binary detection paradigm. However, the selection of an appropriate DI formulation may influence the damage diagnosis performance while the majority of existing methods are deterministic in nature, thus not accounting for various types of uncertainty, and require the use of user-defined arbitrary detection and identification thresholds. To eliminate the limitations of conventional time-domain DIs, improvements have been made by the use of frequency-domain DIs or a combination of time-frequency (mixed-domain) DIs [6], [7]. Recently, steps have been taken towards formulating probabilistic DIs using Gaussian mixture models, Gaussian process regression, and other probabilistic and/or statistical tools [5], [8], [9]. These methods attempt to model the DIs evolution under different damage states and/or classify the structural state based on probabilistic or statistical techniques based on DI obtained under considered damage states. However, they do not model the actual wave propagation for the different paths nor account for the underlying wave propagation dynamics.

Stochastic time series models, inherently accounting for uncertainty, and corresponding statistical methods have been proposed in the context of the vibration-based SHM [10], [11]. In the context of active sensing SHM, ultrasonic guided waves are dispersive in nature, thus non-stationary with variance evolving over time [12], and in order to properly represent them, time-varying parametric time series models are required. Time-varying parametric methods can be based upon parameterized representations of the time-dependent auto-regressive moving average (TARMA) or related types and their extensions. These representations differ from their conventional, stationary, counterparts in that their parameters are time dependent [13], [14].

The main objective of this work is the introduction and ex-

<sup>1</sup>Corresponding author; Email kopsaf@rpi.edu

perimental assessment of a novel damage detection and identification scheme for active sensing SHM based on stochastic time-varying, namely functional-series time-varying autoregressive (FS-TAR) and recursive maximum likelihood time-varying autoregressive (RML-TAR), models. These models are used to represent the guided wave propagation for different actuator-sensor paths on the monitored structure and the estimated time-varying parameters are subsequently used to tackle damage detection and identification within a statistical hypothesis decision making scheme. The parameters of the RML-TAR model are free to evolve with time and no structure is imposed upon them, whereas the parameters of the FS-TAR model are projected onto functional subspaces assuming a deterministic evolution of the wave propagation. It is to be mentioned here that the family of basis functions selected for the projection of the FS-TAR model's time-dependent parameters is of crucial importance. By taking advantage of prior information about the physics of the non-stationary signals or parameter evolution, appropriate families of basis functions (wavelets, trigonometric, polynomial, etc.) can be selected. As guided wave propagation is deterministic in nature, FS-TAR representations constitute a natural choice. To the authors' best of knowledge, this is the first study that explores the use of stochastic time-varying time series models in the context of active sensing acousto-ultrasound-based SHM.

## II. EXPERIMENTAL SETUP AND SIGNALS

In this study, a  $152.4 \times 279.4$  mm ( $6 \times 11$  in) 6061 aluminum coupon ( $2.36$  mm/ $0.093$  in thick) was used (Figure 1a). Using Hysol EA 9394 adhesive, six lead zirconate titanate (PZT) piezoelectric sensors (type PZT-5A, Acellent Technologies, Inc) of  $6.35$  mm ( $1/4$  in) diameter and a thickness of  $0.2$  mm ( $0.0079$  in), were attached to the plate and cured for 24 hrs in room temperature. Figure 1b shows the dimensions of the plate, placement of the PZT transducers, and the path naming convention. After curing, the plate was mounted on a tensile testing machine (Instron, Inc), where five static loading conditions were applied consecutively: 0, 5, 10, 15, and 20 kN. During each loading phase, up to four three-gram weights were taped to the surface of the plate starting from its center point to simulate local damage (Figure 1b).

Narrowband actuation signals in the form of 5-peak tone bursts (5-cycle Hamming-filtered sine wave,  $90$  V peak-to-peak,  $250$  kHz center frequency) were used as actuation for each sensor consecutively. Data was collected using a ScanGenie III data acquisition system (Acellent Technologies, Inc) from selected sensors during each actuation cycle at a sampling frequency of  $24$  MHz. Using this process, 20 signals for each sensor-actuator path (wave propagation path), damage, and loading condition were recorded. This led to a total of 410 data sets for each sensor. For the time-series modeling, the acquired signals were down-sampled to  $2$  MHz. This process resulted in 612-sample-long signals.

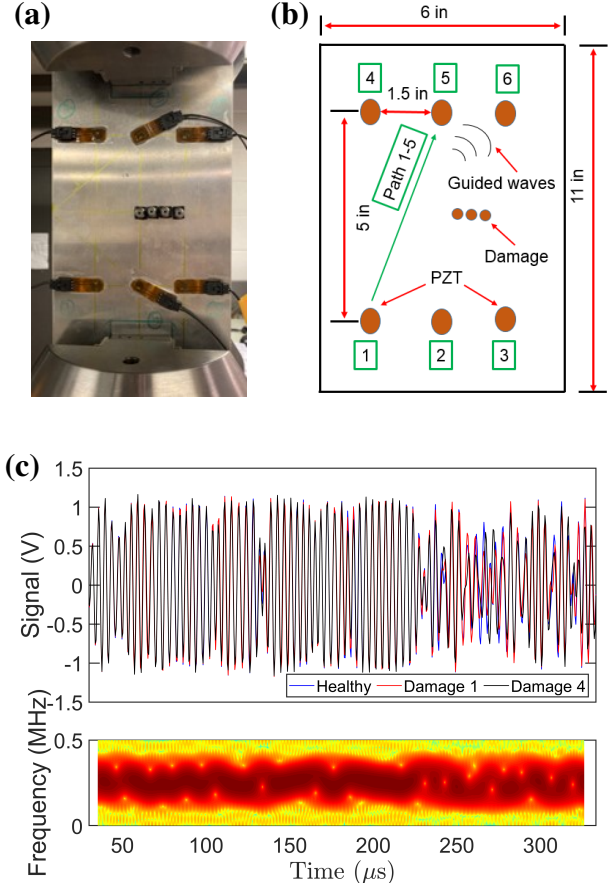


Fig. 1. (a) The plate used in this study installed on the testing machine; (b) schematic of the plate's sensor layout and dimensions; (c) indicative guided wave signals for healthy and damaged cases with a representative non-parametric spectrogram.

Figure 1c presents indicative non-parametric results<sup>1</sup> in the form of the spectrogram that shows the time-varying nature of the wave propagation signal.

## III. STOCHASTIC TIME-VARYING MODELS

Guided waves are inherently non-stationary due to their time-dependent (evolutionary) and dispersive characteristics, and are heavily influenced by environmental and operating conditions. The time-varying nature of guided waves requires the use of corresponding time-varying non-parametric and/or parametric models [13]–[15]. Stochastic parametric non-stationary (time-varying) models such as time-dependent autoregressive (TAR) models, or related types and their extensions, have been mainly used in the context of random vibration analysis [13], [15], [16], with detailed reviews presented in [13], [14]. In this study, the time-varying characteristics of the guided wave signals have been modeled via RML-TAR and FS-TAR models for the purpose of damage detection and identification.

RML-TAR models represent their conventional, stationary AR counterparts with the significant difference being that

<sup>1</sup>window length: 30 samples; 98% overlap; NFFT points: 30000 (zero-padding took place to obtain smooth magnitude estimates); frequency resolution  $\Delta f = 666.66$  Hz.

they allow their parameters to depend upon time and *adapt* based on the time-dependent nature of the wave propagation [13]. An RML-TAR( $na$ ) model, with  $na$  designating its AR order, is thus of the form:

$$y[t] + \sum_{i=1}^{na} a_i[t] \cdot y[t-i] = e[t], \quad e[t] \sim \text{iid } \mathcal{N}(0, \sigma_e^2[t]) \quad (1)$$

with  $t$  designating discrete time,  $y[t]$  the time-varying wave propagation signal to be modeled,  $e[t]$  an (unobservable) uncorrelated (white) Gaussian innovations sequence with zero mean and time-dependent variance  $\sigma_e^2[t]$ . The time-varying AR parameter vector  $\theta[t] = [a_1[t] \ a_2[t] \ \dots \ a_{na}[t]]^T_{[na \times 1]}$  is estimated from the available data.

It can be shown that the minimum mean square error (MMSE) one-step-ahead prediction  $\hat{y}[t/t-1]$  of the signal value  $y[t]$  made at time  $t-1$  (that is for given values of the signal up to time  $t-1$ ) is<sup>2</sup>:

$$\hat{y}[t/t-1] = - \sum_{i=1}^{na} a_i[t] \cdot y[t-i] \quad (2)$$

Comparing this with the Equation (1), it is evident that the one-step-ahead prediction error is equal to  $e[t]$ , that is:

$$\hat{e}[t/t-1] \triangleq y[t] - \hat{y}[t/t-1] = e[t]. \quad (3)$$

In the case of FS-TAR models, a deterministic structure is imposed upon the time evolution of the parameters. This is achieved by postulating model parameters as deterministic functions of time, belonging to specific functional subspaces. The FS-TAR parameters, as well as innovations standard deviations, are all projected onto properly selected functional subspaces:

$$\begin{aligned} \mathcal{F}_{AR} &\triangleq \{G_{b_a(1)}[t], G_{b_a(2)}[t] \dots G_{b_a(p_a)}[t]\} \\ \mathcal{F}_{\sigma_e} &\triangleq \{G_{b_s(1)}[t], G_{b_s(2)}[t] \dots G_{b_s(p_s)}[t]\}. \end{aligned}$$

In these expressions, “ $\mathcal{F}$ ” designates the functional subspace of the indicating quantity and  $G_j[t]$  a set of orthogonal basis functions selected from a suitable family (such as Chebyshev, Legendre, other polynomials, trigonometric, wavelet, or other functions). The AR and standard deviation subspace dimensionalities are indicated as  $p_a$  and  $p_s$ , respectively, while, the indices  $b_a(i)(i = 1, \dots, p_a)$  and  $b_s(i)(i = 1, \dots, p_s)$  designate the specific basis functions of a particular family that are included in each subspace. The time-dependent AR and innovations standard deviation of an FS-TAR( $na$ ) $_{[p_a, p_s]}$  representation may be expressed as:

$$y[t] + \sum_{i=1}^{na} a_i[t] \cdot y[t-i] = e[t], \quad e[t] \sim \text{iid } \mathcal{N}(0, \sigma_e^2[t]) \quad (4)$$

$$a_i[t] \triangleq \sum_{j=1}^{p_a} a_{i,j} \cdot G_{b_a(j)}[t] \quad \sigma_e[t] \triangleq \sum_{j=1}^{p_s} s_j \cdot G_{b_s(j)}[t] \quad (5)$$

with  $a_{i,j}$  and  $s_j$  designating the AR and innovations standard deviation coefficients of

<sup>2</sup>A hat designates estimator/estimate; for instance  $\hat{\theta}$  is an estimator/estimate of  $\theta$ .

projection. The coefficients of projection vector  $\theta = [a_{1,1} \ \dots \ a_{1,pa} \ \dots \ a_{na,1} \ \dots \ a_{na,pa}]^T_{[napa \times 1]}$  has to be estimated from the available data.

#### IV. MODEL IDENTIFICATION

The model identification problem, both for RML-TAR and FS-TAR, is distinguished into two subproblems: (i) *parameter estimation* and (ii) *model structure selection*. In this work, TAR parameter estimation is based on the following exponentially weighted prediction error criterion (incorporating a “forgetting” factor [13]) and a recursive estimation scheme accomplished via the recursive maximum likelihood (RML) method [13], [15]:

$$\hat{\theta}[t] = \arg \min_{\theta[t]} \sum_{\tau=1}^t \lambda^{t-\tau} \cdot e^2[\tau, \theta^{\tau-1}], \quad (6)$$

$$e[t, \theta^{t-1}] \triangleq y[t] - \sum_{i=1}^{na} a_i[t-1] \cdot y[t-i] \approx e[t, \theta^t] \quad (7)$$

where,  $\theta^t$  stands for all AR parameters up to time  $t$ . In these expressions  $\arg \min$  designates minimizing argument, and  $e[t, \theta^{t-1}]$  the model’s one-step-ahead prediction error made at time  $t-1$  without knowing the model parameter values at time  $t$ . As indicated in the expression above,  $e[t, \theta^{t-1}] \approx e[t, \theta^t]$  for slow parameter evolution. The term  $\lambda^{t-\tau}$  is a window or weighting function that for  $\lambda \in (0, 1)$  assigns more weight to more recent errors [15, pp. 378-379]. The quantity  $\lambda$  is referred to as the “forgetting factor”. The smaller the value of  $\lambda$ , the faster older values of the error (and thus the signal) are forgotten, thus increasing the estimator’s adaptability, i.e. its ability to track the evolution of the dynamics.

The recursive estimation of  $\theta[t]$  based upon the above criterion is accomplished via the RML method [13], [15], thus the models are designated as RML-TAR( $na$ ) $_{\lambda}$ . The estimator update at time  $t$  based on the previous time instant  $t-1$  is given as:

$$\hat{\theta}[t] = \hat{\theta}[t-1] + k[t] \cdot \hat{e}[t|t-1] \quad (8)$$

with  $\hat{e}[t|t-1]$  designating the prediction error:

$$\hat{e}[t|t-1] = y[t] - \hat{y}[t|t-1] = y[t] - \phi^T[t] \cdot \hat{\theta}[t-1] \quad (9)$$

and  $k[t]$  the adaptation gain:

$$k[t] = \frac{\mathbf{P}[t-1] \cdot \phi[t]}{\lambda + \phi^T[t] \cdot \mathbf{P}[t-1] \cdot \phi[t]} \quad (10)$$

In equation (10),  $\mathbf{P}[t]$  designates the parameter covariance matrix at time  $t$  that is updated based on the following recursive form:

$$\mathbf{P}[t] = \frac{1}{\lambda} \left[ \mathbf{P}[t-1] - \frac{\mathbf{P}[t-1] \cdot \phi[t] \cdot \phi^T[t] \cdot \mathbf{P}[t-1]}{\lambda + \phi^T[t] \cdot \mathbf{P}[t-1] \cdot \phi[t]} \right] \quad (11)$$

with  $\phi[t]$  corresponding to the regression vector, defined as:

$$\phi[t] = [-y[t-1] \ -y[t-2] \ \dots \ -y[t-na]].$$

In the case of FS-TAR models, in order to estimate the coefficients of projection vector  $\vartheta$  from the available data, Equation (4) and Equation (5) can be recast in the following form [13], [17], [18]:

$$y[t] = \phi^T[t] \cdot \vartheta + e[t, \vartheta] \quad (12)$$

with

$$\phi^T[t] \triangleq [-G_{b_a(1)}[t]y[t-1] \dots -G_{b_a(pa)}[t]y[t-na]]^T \quad (13)$$

Estimation of the coefficients of projection vector  $\vartheta$  of the FS-TAR model may be based upon a prediction error criterion (PE) consisting of the sum of squares of the model's one-step-ahead prediction errors (residual sum of squares):

$$\hat{\vartheta} = \arg \min_{\vartheta} \sum_{t=1}^N e^2[t, \vartheta]. \quad (14)$$

Since the residual  $e[t, \vartheta]$  depends linearly upon the coefficient of projection vector  $\vartheta$ , minimization of the PE criterion of Equation (14) leads to the ordinary least squares (OLS) or weighted least squares (WLS) estimators. Alternatively, ML estimation can be also used. For details see [13], [14]. The estimation of the innovations standard deviation coefficients of projection may be achieved as described in [18].

The associated covariance matrix for the estimated coefficient of projection vector  $\vartheta$  can be obtained as [18]:

$$P_{\vartheta} = \frac{1}{N} \cdot \left\{ \frac{1}{N} \sum_{t=1}^N \frac{\phi_A[t] \cdot \phi_A^T[t]}{(\mathbf{g}_s^T[t] \cdot \hat{s}^{ML})^2} \right\}^{-1} \cdot \left\{ \frac{1}{N} \sum_{t=1}^N \frac{\sigma_e^2[t] \cdot \phi_A[t] \cdot \phi_A^T[t]}{(\mathbf{g}_s^T[t] \cdot \hat{s}^{ML})^4} \right\} \cdot \left\{ \frac{1}{N} \sum_{t=1}^N \frac{\phi_A[t] \cdot \phi_A^T[t]}{(\mathbf{g}_s^T[t] \cdot \hat{s}^{ML})^2} \right\}^{-1}$$

Notice that the covariance matrix  $P_{\vartheta}$  for the coefficients of projection vector  $\vartheta$  is not time-varying. In order to perform damage detection and identification, time-varying parameters and the associated time-varying covariance matrix  $P[t]$  would be necessary. The time-varying parameter vector  $\theta[t] = [a_1[t] \ a_2[t] \ \dots \ a_{na}[t]]$  can be obtained via Equation (5). The associated time-varying covariance matrix can be obtained by following three steps: (i) sample  $m$ -times from a multivariate Gaussian distribution with mean  $\vartheta$  and covariance  $P_{\vartheta}$  ( $\mathcal{N}(\vartheta, P_{\vartheta})$ ); (ii) obtain the associated time-varying parameters  $\theta[t]$  from Equation (5) to obtain  $m$ -realizations of the parameters; (iii) estimate the sample mean  $\theta[t]$  and covariance  $P[t]$ .

## V. DAMAGE DETECTION AND IDENTIFICATION

Damage detection and identification can be based on a characteristic quantity  $Q[t] = f(\theta[t])$ , where  $\theta[t]$  is a function of the parameter vector from the RML-TAR or FS-TAR models. Let  $\hat{\theta}[t]$  designate a proper estimator of the parameter vector  $\theta[t]$ . For a sufficiently long signal, the

estimator is (under mild assumptions) Gaussian distributed with mean equal to its true value  $\theta[t]$  and a certain covariance  $P[t]$ . Hence  $\hat{\theta}[t] \sim \mathcal{N}(\theta[t], P[t])$ . Damage detection is based on testing for statistically significant changes in the parameter vector  $\theta[t]$  between the nominal and current state of the structure through a hypothesis testing problem:

$$H_0[t] : \delta\theta[t] = \theta_o[t] - \theta_u[t] = 0$$

null hypothesis–healthy structure

$$H_1[t] : \delta\theta[t] = \theta_o[t] - \theta_u[t] \neq 0$$

alternative hypothesis – damaged structure

The difference between the two parameter vector estimators follows Gaussian distribution, that is,  $\delta\hat{\theta}[t] = \hat{\theta}_o[t] - \hat{\theta}_u[t] \sim \mathcal{N}(\delta\theta[t], \delta P[t])$ , with  $\delta\theta[t] = \theta_o[t] - \theta_u[t]$  and  $\delta P[t] = P_o[t] + P_u[t]$ , where  $P_o[t]$ ,  $P_u[t]$  designate the corresponding time-varying covariance matrices. Under the null ( $H_0[t]$ ) hypothesis  $\delta\hat{\theta}[t] = \hat{\theta}_o[t] - \hat{\theta}_u[t] \sim \mathcal{N}(0, 2P_o[t])$  and the quantity

$$Q[t] = (\delta\hat{\theta}[t])^T \cdot \delta P[t]^{-1} \cdot \delta\hat{\theta}[t], \quad \delta P[t] = 2P_o[t] \quad (15)$$

follows a  $\chi^2$  distribution with  $d = \dim(\theta[t])$  (parameter vector dimensionality) degrees of freedom. As the time-varying covariance matrix  $P_o[t]$  corresponding to the healthy structure is unavailable, its estimated version  $\hat{P}_o[t]$  is used. Then the following test is constructed at the  $\alpha$  (type I) risk level:

$$Q[t] \leq \chi^2_{1-\alpha}(d) \implies H_0[t] \text{ is accepted} \quad (16)$$

$$\text{Else} \implies H_1[t] \text{ is accepted} \quad (17)$$

where,  $\chi^2_{1-\alpha}(d)$  designates the  $\chi^2$  distribution's  $(1 - \alpha)$  critical points. Damage identification may be based on a multiple hypothesis testing problem comparing the parameter vector  $\hat{\theta}_u[t]$  belonging to the current structural state to those corresponding to different damage types  $\hat{\theta}_A[t]$ ,  $\hat{\theta}_B[t]$ , ... .

## VI. RESULTS AND DISCUSSION

In the present study, Figure 1(b) shows the actuator-sensor layout, and six sensors/actuators have been used. Damage starts from the center of the plate and grows in magnitude to the right. In this study, simulated damages have been used in the form of weights mounted to the plate with tacky tapes. It has been shown that when the guided wave crosses the damage (referred to as damage-intersecting path), a significant change can be observed in the signal with the increase in damage size. On the other hand, for a damage non-intersecting path, one can observe that the received signals sustain significantly smaller changes with the increase in damage size. Thus, damage non-intersecting paths naturally carry less information when it comes to damage detection and identification compared to damage-intersecting paths. In this work, the following time-domain DI is employed as a reference in order to compare the performance of the DI-based approach and the time series model-based approach proposed herein. The DI used was adopted from the work of Janapati et al. [19]. Given a baseline signal  $y_o[t]$  and an

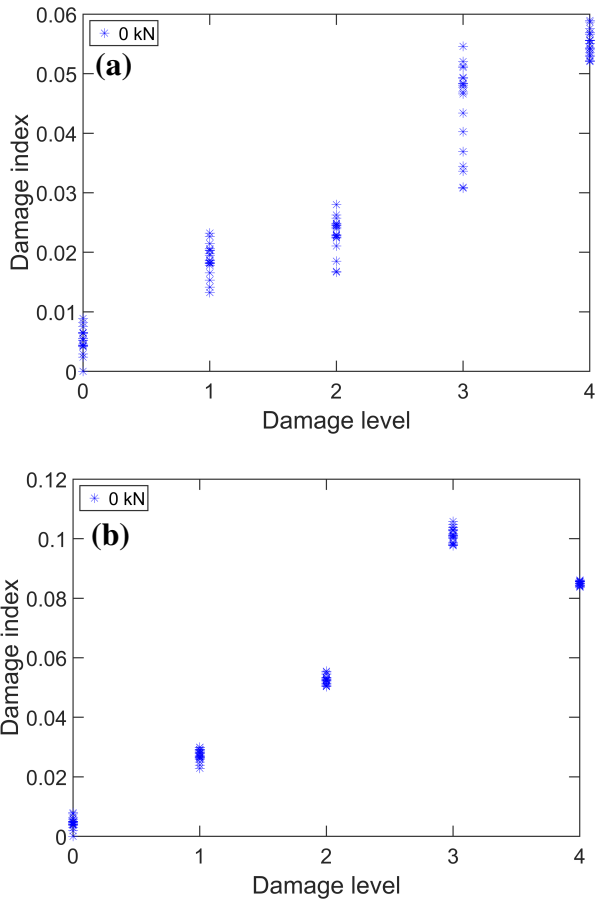


Fig. 2. The evolution of the damage index [19] as applied to indicative actuator-sensor paths: (a) damage non-intersecting path 1-4; and (b) damage intersecting path 2-6.

unknown signal  $y_u[t]$  indexed with normalized discrete time  $t(t = 1, 2, 3, \dots, N)$  where  $N$  is the number of data samples considered in the calculation of the DI, the formulation of that DI is as follows:

$$Y_u^n[t] = \frac{y_u[t]}{\sqrt{\sum_{t=1}^N y_u^2[t]}} \quad (18)$$

$$Y_o^n[t] = \frac{y_o[t] \cdot \sum_{t=1}^N (y_o[t] \cdot Y_u^n[t])}{\sum_{t=1}^N y_o^2[t]} \quad (19)$$

$$\text{DI} = \sum_{t=1}^N (Y_u^n[t] - Y_o^n[t])^2 \quad (20)$$

In this notation,  $Y_u^n[t]$  and  $Y_o^n[t]$  are normalized unknown (inspection) and baseline signals, respectively.

Figures 2(a) and (b) show the evolution of the DI with increasing damage size for a damage non-intersecting path and intersecting path, respectively. It can be observed that the magnitude of the DI for the damage non-intersecting path is much smaller than the damage intersecting path. Damage detection and identification can be based upon the definition of appropriate thresholds that can be based on historical data

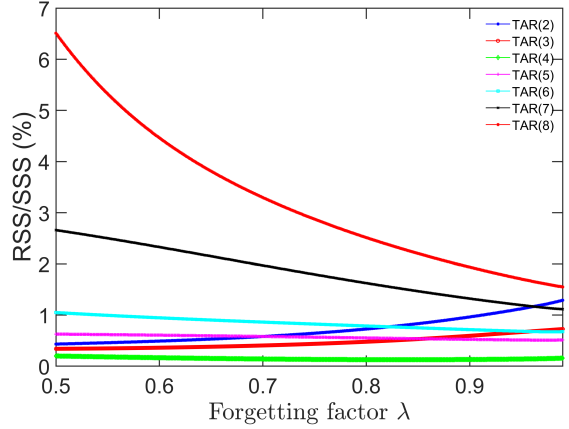


Fig. 3. Model structure selection of the healthy structure using RML-TAR model for path 2-6: the RSS/SSS versus the forgetting factor values for different model orders are shown.

and/or user experience.

In order to detect and identify damage using stochastic time-varying time series models, it is first necessary to identify the system in its healthy state while the guided wave signals are being propagated for each path. Figure 3 shows the RML-TAR model identification process of the structure in its healthy states for path 2-6.

Model selection of RML-TAR involves selecting the appropriate model order  $na$  and forgetting factor  $\lambda$ . The RSS/SSS (Residual Sum of Squares/Signal Sum of Squares) criterion, describing the predictive ability of the model, was employed for the model selection process. AR orders from  $na = 2$  to  $na = 22$  and forgetting factor values  $\lambda \in [0.5, 0.999]$  (with an incremental step of 0.001) were considered to create a pool of candidate models. A total of 10,500 models ( $500 \times 21$ ) were estimated, and among all these models, the best model was chosen as the one that minimizes the RSS/SSS. Following this criterion, the best model occurred for  $na = 4$  and forgetting factor  $\lambda = 0.835$  (Figure 3). This can be compactly represented as RML-TAR(4)<sub>0.835</sub>. In addition to the RSS/SSS criterion, the Bayesian Information Criterion (BIC), which rewards the model's predictive capability while penalizing model complexity for increasing model order [13] was also taken into account. Model validation took place via examination of the whiteness, or uncorrelatedness, normality hypothesis of the model residuals as well as the residual sign test. Following the same process, for path 1-4, the best model occurred for RML-TAR(6)<sub>0.993</sub>. It is to be mentioned here that, although with the forgetting factor 0.835 and 0.993, the models had the lowest RSS/SSS and are necessary for extracting the modal properties of the system, however, in the context of damage detection and identification, the use of a forgetting factor 1 simplifies the model and the subsequent analysis. For this reason, RML-TAR(4)<sub>1</sub> was used for the subsequent analysis.

Model selection of FS-TAR involves selecting the appropriate AR order  $na$  and the functional subspaces  $\mathcal{F}_{AR}$  and

$\mathcal{F}_{\sigma_e}$ . In the present case, the best FS-TAR model minimizes the BIC criteria utilizing an integer optimization scheme as described in [13], [18]. The integer optimization scheme utilizes coarse optimization based upon a genetic algorithm (population size 100, number of generations 100, crossover probability 0.8 and mutation probability 0.05) and fine optimization based upon the concept of backward regression. The functional subspaces considered are trigonometric functions. For path 2-6, the best model occurred for  $na = 4$  and the functional subspaces are  $\mathcal{F}_{AR} = \{G_1[t], G_6[t], G_8[t]\}$  ( $pa = 3$ ) and  $\mathcal{F}_{\sigma_e} = \{G_1[t], G_2[t], G_3[t]\}$  ( $ps = 3$ ). This is compactly written as FS-TAR(4)<sub>[3,3]</sub>. Similarly, for path 1-4, the best model occurred for  $na = 4$  and  $\mathcal{F}_{AR} = \{G_1[t], G_3[t], G_4[t], G_9[t]\}$  ( $pa = 4$ ) and  $\mathcal{F}_{\sigma_e} = \{G_1[t], G_2[t], G_4[t]\}$  ( $ps = 3$ ) compactly written as FS-TAR(4)<sub>[4,3]</sub>. Maximum-likelihood estimator was used for estimating the coefficients of projection vector  $\vartheta$ .

Figure 4 depicts the time-varying model parameters of the RML-TAR model for damage intersecting path 2-6. The solid lines represent the mean parameter values and the shaded regions represent the  $\pm 2$  standard deviation confidence intervals for each state derived from the corresponding experimental realizations. Figure 5 shows the RML-TAR(4)<sub>1</sub> model based time-varying damage detection for damage non-intersecting path 1-4 and damage intersecting path 2-6. In this case, the model-based covariance matrix was used (Equation 11). Note that for damage intersecting path 2-6 (Figure 5(b)), perfect damage detection is possible. The dotted red line is the critical value of the characteristic quantity  $Q[t]$  and the degrees of freedom  $d = 4$ . All the damaged states are outside this critical value. However, for damage non-intersecting path 1-4, only damage level 2,3 and 4 are detected as they go outside this critical value (adjusted  $\alpha$ ). It should be noted here that better damage detection is possible if the covariance matrix is derived from the 20 experimental healthy realizations (gives a tighter bound than the theory). It is also possible to adjust the forgetting factor  $\lambda$  to achieve better damage detection.

Figure 6 shows the time-varying model parameters of the FS-TAR(4)<sub>[3,3]</sub> model for damage intersecting path 2-6. In this case, the model parameters from different states have been plotted together for 100 experimental signals. It can be observed that the model parameters of different states form a band and can be distinguished from each other. From Figure 7, it can be observed that using FS-TAR model, perfect damage detection is possible both for damage non-intersecting path 1-4 (Figure 7(a)) and damage intersecting path 2-6 (Figure 7(b)). The dotted red line is the limiting value or the threshold, and was manually adjusted in this case as the  $\alpha$ -level exceeds the numerical limit. Note that the healthy cases remain completely within the limit for all time instants. However, damage level 1, 2, and 3 are very closely spaced in this case as model-based covariance matrix was used for estimating the time-varying characteristic quantity  $Q[t]$  from Equation 15. This situation can be improved when the covariance matrix is estimated from the experimental realizations of the guided wave signals during the healthy

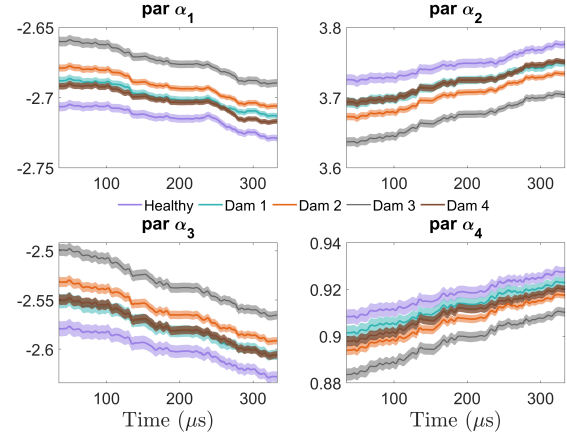


Fig. 4. RML-TAR(4)<sub>1</sub> model parameter variation with time: the solid lines represent the mean parameters and the shaded regions represent the 95% confidence intervals derived from 20 experimental signals from each states, namely: healthy, damage level 1(1 weights), damage level 2 (2 weights), damage level 3 (3 weights), and damage level 4 (4 weights).

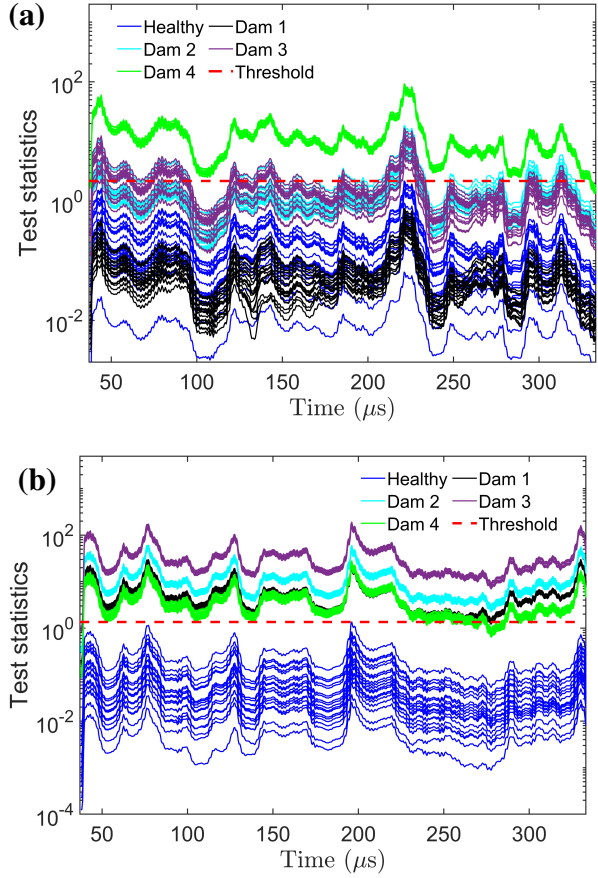


Fig. 5. Time-varying damage detection performance of the RML-TAR(4)<sub>1</sub> model using the model-based covariance matrix: (a) for damage non-intersecting path 1-4; and (b) damage intersecting path 2-6.

state of the structure.

Figure 8 illustrates the damage detection performance of the damage non-intersecting path 1-4 (Figure 8(a)) and damage intersecting path 2-6 (Figure 8(b)) when experimental

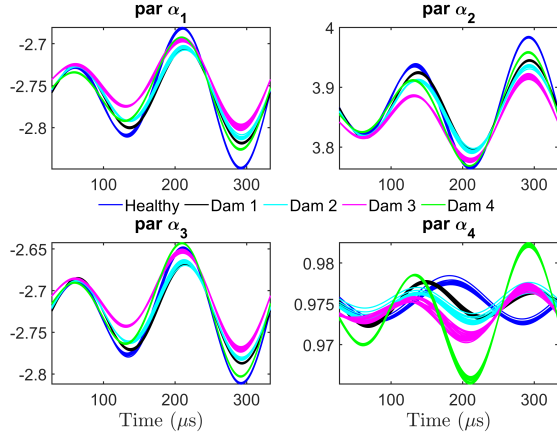


Fig. 6. FS-TAR parameter variation with time for damage intersecting path 2-6: parameters from all 5 states, namely: healthy, damage level 1, damage level 2, damage level 3 and damage level 4 have been plotted together for all 100 signals.

covariance matrix was used in estimating the time-varying characteristic quantity  $Q[t]$  for the FS-TAR model. Note that, perfect damage detection is achieved and different damaged states are well separated from the healthy state. The  $\alpha$ -level used was  $\alpha = 0.001$  with the degrees of freedom  $na \cdot pa = 12$  for damage non-intersecting path 1-4. For damage intersecting path 2-6, the threshold was adjusted as  $\alpha = 0.001$  with the degrees of freedom  $na \cdot pa = 9$ .

Figure 9 shows the performance of the FS-TAR model for damage detection under uncertainty. The baseline signals (healthy state) and all the damaged states signals are for 0 kN load. Then 20 signals were acquired under 5 kN applied load under healthy condition and the proposed algorithm was applied. Note that in this case, the threshold was set at 5 kN load. The test statistics of the healthy signal and the 5 kN load signals lie below the threshold and all other damaged states go outside the threshold. And as such, perfect damage detection is achieved using the FS-TAR model under uncertainty. The  $\alpha$ -level was manually adjusted in this case.

## VII. CONCLUSIONS

The objective of this work was the formulation and experimental assessment of a statistical damage diagnosis scheme in the context of ultrasonic guided wave-based damage diagnosis using two types of parametric stochastic time-varying time series models, namely RML-TAR and FS-TAR. In the RML-TAR formulation, the model parameters evolve in an unstructured way, that is, no specific structure is imposed on their time evolution. However, in the FS-TAR formulation, model parameters evolve in a deterministic way as they are projected onto appropriate functional subspaces. The model parameters were used to diagnose damage based on the definition of statistical quantities and corresponding hypothesis testing procedures. The results of this study indicated that the RML-TAR models can detect damage for damage intersecting paths quite well but fail to do so for damage non-intersecting paths. On the other hand, FS-TAR

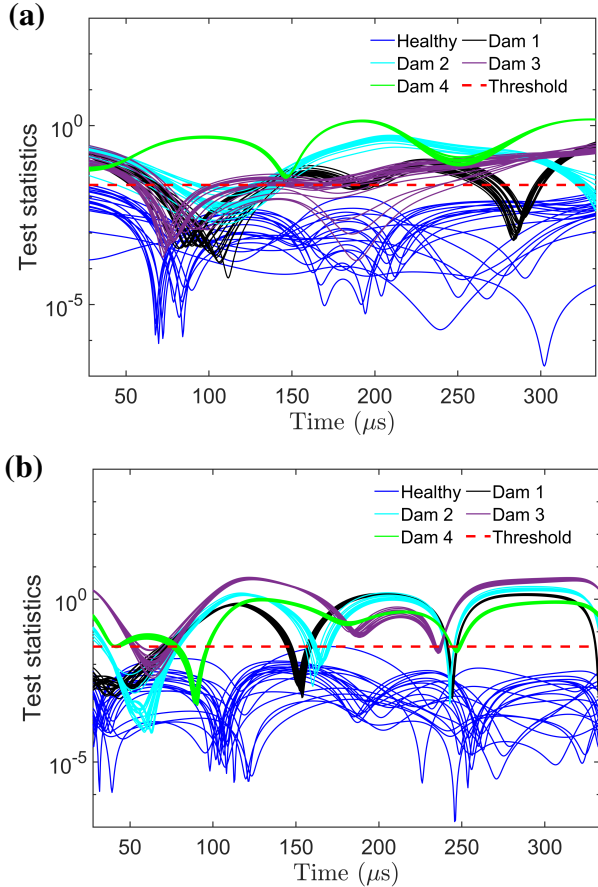


Fig. 7. Time-varying damage detection performance of the FS-TAR model using the model-based covariance matrix: (a) for damage non-intersecting path 1-4; and (b) damage intersecting path 2-6.

models were capable of detecting and classifying damage both for damage intersecting and non-intersecting paths. That is, FS-TAR models were shown to be more sensitive and robust when tackling damage detection.

## ACKNOWLEDGMENT

This work is carried out under the support of the U.S. Air Force Office of Scientific Research (AFOSR) grant “Formal Verification of Stochastic State Awareness for Dynamic Data-Driven Intelligent Aerospace Systems” (FA9550-19-1-0054) with Program Officer Dr. Erik Blasch.

## REFERENCES

- [1] F. Kopsaftopoulos and F.-K. Chang, “A dynamic data-driven stochastic state-awareness framework for the next generation of bio-inspired fly-by-feel aerospace vehicles,” in *Handbook of Dynamic Data Driven Applications Systems*, E. Blasch, S. Ravela, and A. Aved, Eds. Cham: Springer International Publishing, 2018, pp. 697–721.
- [2] C. R. Farrar and K. Worden, “An introduction to Structural Health Monitoring,” *The Royal Society – Philosophical Transactions: Mathematical, Physical and Engineering Sciences*, vol. 365, pp. 303–315, 2007.
- [3] S. Ahmed and F. P. Kopsaftopoulos, “Uncertainty quantification of guided waves propagation for active sensing structural health monitoring,” in *Proceedings of the Vertical Flight Society 75th Annual Forum & Technology Display*, Philadelphia, PA, USA, May 2019.

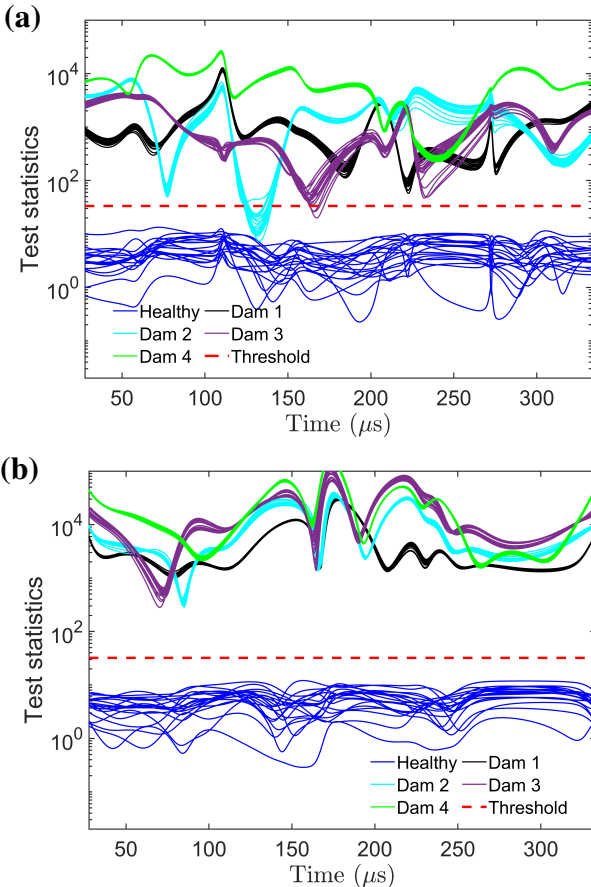


Fig. 8. Time-varying damage detection performance of the FS-TAR model using the covariance matrix derived from the 20 experimental healthy signals: (a) for damage non-intersecting path 1-4; and (b) damage intersecting path 2-6.

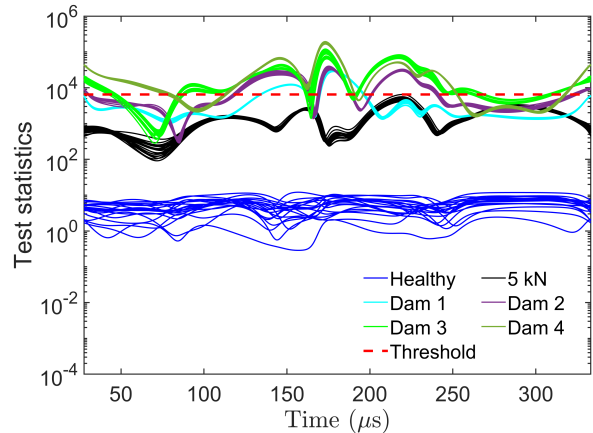


Fig. 9. Time-varying damage detection performance of the FS-TAR model under uncertainty (5 kN applied load) using the covariance matrix derived from the 20 experimental healthy signals for the damage intersecting path 2-6.

interrogation,” *Structural Health Monitoring*, vol. 12, no. 2, pp. 141–152, 2013.

- [10] F. P. Kopsaftopoulos and S. D. Fassois, “A stochastic functional model based method for vibration based damage detection, localization, and magnitude estimation,” *Mechanical Systems and Signal Processing*, vol. 39, no. 1–2, pp. 143–161, August–September 2013.
- [11] F. Kopsaftopoulos and S. Fassois, “Vibration based health monitoring for a lightweight truss structure: experimental assessment of several statistical time series methods,” *Mechanical Systems and Signal Processing*, vol. 24, no. 7, pp. 1977–1997, 2010.
- [12] S. Ahmed and F. Kopsaftopoulos, “Stochastic identification of guided wave propagation under ambient temperature via non-stationary time series models,” *Sensors*, vol. 21, no. 16, 2021. [Online]. Available: <https://www.mdpi.com/1424-8220/21/16/5672>
- [13] A. Pouliomenos and S. Fassois, “Parametric time-domain methods for non-stationary random vibration modelling and analysis—a critical survey and comparison,” *Mechanical systems and signal processing*, vol. 20, no. 4, pp. 763–816, 2006.
- [14] M. Spiridonakos and S. Fassois, “Non-stationary random vibration modelling and analysis via functional series time-dependent arma (fs-tarma) models—a critical survey,” *Mechanical Systems and Signal Processing*, vol. 47, no. 1–2, pp. 175–224, 2014.
- [15] L. Ljung, “System identification: Theory for the user,” 1999.
- [16] D. Sotiriou, F. Kopsaftopoulos, and S. Fassois, “An adaptive time-series probabilistic framework for 4-d trajectory conformance monitoring,” *IEEE Transactions on Intelligent Transportation Systems*, vol. 17, no. 6, pp. 1606–1616, 2016.
- [17] A. G. Pouliomenos and S. D. Fassois, “Output-only stochastic identification of a time-varying structure via functional series tarma models,” *Mechanical Systems and Signal Processing*, vol. 23, no. 4, pp. 1180–1204, 2009.
- [18] M. Spiridonakos and S. Fassois, “An fs-tar based method for vibration-response-based fault diagnosis in stochastic time-varying structures: experimental application to a pick-and-place mechanism,” *Mechanical Systems and Signal Processing*, vol. 38, no. 1, pp. 206–222, 2013.
- [19] V. Janapati, F. Kopsaftopoulos, F. Li, S. J. Lee, and F.-K. Chang, “Damage detection sensitivity characterization of acousto-ultrasound-based structural health monitoring techniques,” *Structural Health Monitoring*, vol. 15, no. 2, pp. 143–161, 2016.